Blue-Phase Liquid Crystals for Projection Displays

Linghui Rao[1,2], Sihui He[1], and Shin-Tson Wu[1]
[1]College of Optics and Photonics, University of Central Florida, Orlando, FL 32816, USA
[2]Syndiant Inc., Dallas, TX 75252, USA

Abstract
A projection display using blue-phase liquid crystal (BPLC) is proposed. The fast-response BPLC enables field sequential projection display with suppressed color breakup. Methods for reducing the operating voltage are also discussed.

Author Keywords
blue-phase liquid crystal; field-sequential; projection display

1. Introduction
Field sequential projection displays with reflective liquid-crystal-on-silicon (LCoS) require a fast response time [1,2]. Nowadays, twisted-nematic cell [3], mixed-mode twisted-nematic cell [4], and vertical alignment nematic cell [5], have been commonly employed in the reflective LCoS projectors. With the thin cell gap approach [6], the response time can be largely reduced; however, it is fairly difficult to control the cell gap uniformity when the cell gap is decreased to around 1 μm. Moreover, the accurate control of the uniformity of the LC alignment layer is also needed for these approaches mentioned above.

Recently, blue-phase liquid crystals (BPLCs) based on the Kerr effect is emerging for direct-view [7-9] and projection displays [10, 11] due to its submillisecond gray-to-gray response time, alignment-layer-free process, and cell gap insensitivity when an in-plane switching (IPS) electrode is used.

In this paper, we present a field sequential projection display using reflective BPLC IPS cell. To lower the driving voltage, a reflective BPLC cell with patterned electrodes IPS structure is proposed. In addition, the wavelength dispersion issue is also discussed.

2. Device Structure
Kerr effect is a type of quadratic electro-optic effect caused by an electric-field-induced ordering of polar molecules in an optically isotropic medium. With no voltage applied, the BPLC medium appears optically isotropic; when an electric field is applied, it becomes optically anisotropic. The induced birefringence (Δn) is related to the electric field (E) as [8,9]:

$$\Delta n_{ind} = \lambda K E^2, \quad (1)$$

where λ is the wavelength and K is the Kerr constant. However, the induced birefringence cannot exceed the maximum birefringence of the host LC composite.

Figure 1 depicts the proposed field sequential reflective projection display with a traditional planar IPS BPLC cell. Here w is the electrode width, l is the spacing between the electrodes, and d is the cell gap. In this system, the light passes the polarization beam splitter (PBS) twice. After the unpolarized light enters the PBS, only the s-polarized light is reflected from the splitter coating and emerges from the bottom of the cube to illuminate the reflective BPLCD. The horizontal fringe fields generated from IPS electrodes introduce phase retardation to the s-polarized incident light. Thus, the s-polarized incident light is converted to the p-polarized light so that it can pass the PBS to the projection screen. In the reflective BPLCD cell, we use Aluminum as the metal reflector. To avoid the voltage shielding effect from the metal reflector, there is a passivation layer on top of the metal.

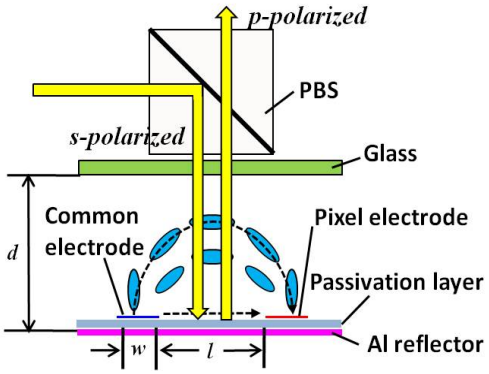

Figure 1. Device structure of the reflective BPLC projection display.

3. Experiment
In the experiment, we have prepared a BPLC IPS cell (IPS 10-10) with electrode width w=10 μm, gap length l=10 μm, and cell gap d=7.5 μm. The BPLC material is JC-BP01M [12]. At ~25°C, we measured the voltage-dependent transmittance (VT) curve at the transmissive mode and the voltage-dependent reflectance (VR) curve at the reflective mode with a He-Ne laser (λ=633 nm). The measured results are shown with solid lines in Fig. 2. From the fitting to the transmittance curve, we obtained the Kerr constant K=10.82 nm/V^2. With the same Kerr constant, we also calculated the VR curve and it fits very well with the experimental result. The dashed lines in Fig. 2 are the fitting results. Compared to the transmissive mode, the reflective mode bares a much lower driving voltage as the incident light accumulates twice the phase retardation through the double pass. However, with an IPS 10-10 cell, the on-state voltage (V_{on}) for the reflective mode is still as high as 36 volts.

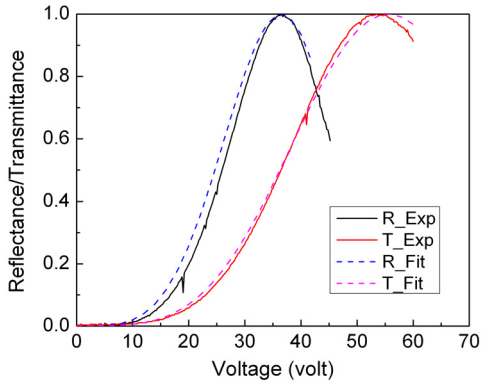

Figure 2. VT & VR curves of the BPLC IPS cell, w=10 μm, l=10 μm, and d=7.5 μm cell at λ=633 nm. Solid lines are experimental results and dashed lines are fitting curves.

 ISSN 0097-966X/13/4402-0902-$1.00

We have also measured the response time for the reflective mode IPS 10-10 BPLCD. The fall time is 1.3 ms. For the same LC cell, if we measure it in the transmissive mode, the fall time is 2.3 ms. The reason is that V_{on} of the reflective mode is much lower. The response time becomes slower as the applied electric field exceeds a critical field (E_c) [13]. When $E>E_c$, electrostriction effect-induced lattice distortion would occur, which not only slow down the response time but also cause hysteresis [14, 15]. The critical field depends on the BPLC materials. Semi-empirically, the critical field is related to the Kerr constant of the BPLC material as [13]:

$$E_c \propto 1/\sqrt{K}. \quad (2)$$

That means, a larger-K BPLC material would also have a lower critical field.

4. Simulation Results and Discussions

To lower the operating voltage, we could decrease the electrode gap l so that the electric field would be stronger for a given applied voltage. We have calculated the VR curves of reflective IPS BPLCD with w=2 μm, l=4 μm (figure is not shown here). Compared to IPS-10/10 whose V_{on}=36 volts [Fig. 2], the V_{on} for IPS-2/4 at λ=650nm is reduced to 26.4 V_{rms}. Due to the wavelength dispersion of Kerr constant [16], V_{on} for green (550nm) and blue (450nm) are reduced to 22 volts and 18.2 volts.

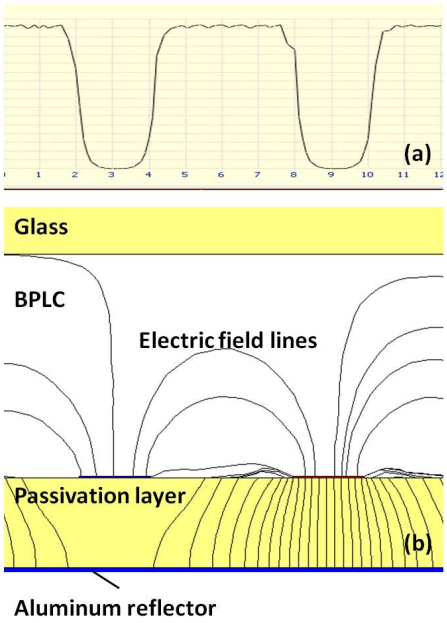

Figure 3. (a) Reflectance distribution and (b) electric field distribution in the reflective IPS BPLCD. Cell: IPS 2-4, wavelength: 650nm, applied voltage: 26.4 volts (V_{on}).

Figures 3(a) and 3(b) are the reflectance and electric field distribution in the reflective BPLCD (IPS 2-4) with an applied voltage of 26.4 volts (V_{on}) at λ=650nm. The reflectance peaks at the gap area between the electrodes. The electric fields on top of the electrodes are in the vertical direction therefore the area on top of the electrodes does not contribute to the reflectance. From Fig. 3(b), the lateral fields are affected by the aluminum reflector which will potentially decrease the optical efficiency. A typical passivation layer thickness is 0.5μm to 1μm (SiO_2), which is sufficient to reduce the electric field bending effect. From simulation, the optical efficiency with the passivation layer is only ~5% lower than the ideal case.

To further decrease the operating voltage, various patterned electrodes [17-20] and vertical field switching [21-23] have been proposed. Figure 4 shows the simulated VR curves of the reflective BPLC cell with protrusion electrodes at different wavelengths. Inset is the structure of the protrusion electrodes. The dimension of the trapezoid electrode structure is defined as follows: w_1 is the bottom width, w_2 is the top width, h is the height, and l is the space between the electrodes. In this simulation, w_1=2 μm, w_2=1 μm, h=2 μm, and l=4 μm. With the patterned electrodes, the electric field is stronger and it penetrates deeper into the BPLC bulk region. Therefore, V_{on} for red (650nm), blue (550nm) and green (450nm) colors are decreased to 13.8 volts, 11.8 volts and 10 volts, respectively.

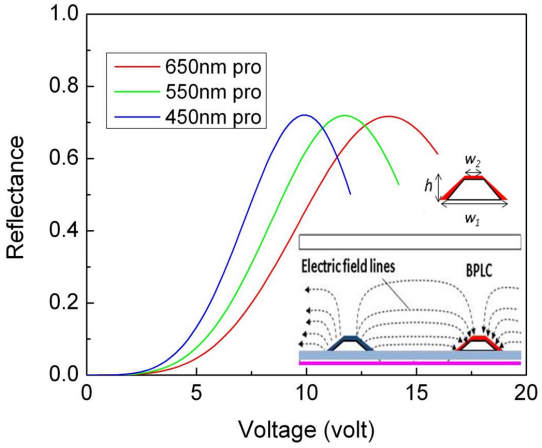

Figure 4. Simulated VR curves of the reflective BPLC cell with protrusion electrodes at different wavelengths. Inset is the structure of the reflective BPLCD with the protrusion electrodes.

From Fig. 4, the wavelength dispersion of the VR curves is quite different from that of a nematic IPS cell. The reasons are explained as follows. In a nematic IPS cell, both top and bottom substrates have strong anchoring energy originated from rubbing. At a given voltage, the electric field strength decreases gradually from the bottom substrate (IPS electrodes) to the top. As a result, double TN cells with reversed twists are formed [24]. Due to polarization rotation effect, the TN cells are inert to the wavelength. However, in a BPLC cell, there is no surface rubbing. Moreover, the Kerr constant of a BPLC material is wavelength dependent as [9]:

$$\lambda K = G\frac{\lambda^2\lambda^{*2}}{\lambda^2-\lambda^{*2}}, \quad (2)$$

here λ^* is the mean resonance wavelength and G is a proportionality constant. Therefore, the VT/VR curves of an IPS-based BPLC are similar to those of a VAN cell. Also noticed from Fig. 4, the peak reflectance of the BPLC cell is only 72%. This is because of the dead zones above the IPS electrodes, as Figs. 3(a) shows. However, in experiment the transmittance could reach 85%–90% because of the dielectric coupling effect [25]. This dielectric coupling effect helps to reorient the BPLC near the electrode edges so that the effective aperture ratio is increased. A tradeoff is in the slightly higher

voltage. This optical efficiency is comparable to that of VAN mode after having considered the fringing field effect.

5. Conclusion

We proposed a color-sequential projection display using reflective mode polymer-stabilized BPLCD. The fast response time of BPLC enables color-sequential technique to be implemented for LCoS projector. The alignment-layer-free feature of in BPLCD simplifies the fabrication process. Low voltage design and wavelength dispersion issue is also discussed.

6. References

[1] M. S. Brennesholtz and E. H. Stupp, Projection Displays, 2nd Ed. (Wiley, 2008).

[2] D. Armitage, I. Underwood and S. T. Wu, "Introduction to Microdisplays" (Wiley, 2006).

[3] M. Schadt and W. Helfrich, "Voltage-dependent optical activity of a twisted nematic liquid crystal," *Appl. Phys. Lett.* **18**, 127–128 (1971).

[4] S. T. Wu and C. S. Wu, "Mixed mode twisted nematic liquid crystal cells for reflective displays," *Appl. Phys. Lett.* **68**, 1455-1457 (1996).

[5] H. D. Smet, D. Cuypers, A. V. Calster, J. V. Steen, and G. V. Doorselaer, Design, fabrication and evaluation of a high-performance XGA VAN-LCOS microdisplay," *Displays* **23**, 89–98 (2002).

[6] S. Gauza, X. Zhu, S. T. Wu, W. Piecek, and R. Dabrowski, "Fast-switching liquid crystals for color-sequential LCDs," *J. Display Technol.* **3**, 250-252 (2007).

[7] H. Kikuchi, M. Yokota, Y. Hiskado, H. Yang, and T. Kajiyama, "Polymer-stabilized liquid crystal blue phases," *Nat. Mater.* **1**, 64–68 (2002).

[8] Z. Ge, S. Gauza, M. Jiao, H. Xianyu, and S. T. Wu, "Electro-optics of polymer-stabilized blue phase liquid crystal displays," *Appl. Phys. Lett.* **94**, 101104 (2009).

[9] Z. Ge, L. Rao, S. Gauza, and S. T. Wu, "Modeling of blue phase liquid crystal displays," *J. Display Technol*. **5**, 250-256 (2009).

[10] S. He, J. H. Lee, H. C. Cheng, J. Yan, and S. T. Wu, "Fast-response blue-phase liquid crystal for color-sequential projection displays," *J. Display Technol.* **8**, 352-356 (2012).

[11] L. Rao, S. He, and S. T. Wu, "Blue-phase liquid crystals for reflective projection displays," *J. Display Technol.* **8**, 555-557 (2012).

[12] L. Rao, J. Yan, and S. T. Wu, "A large Kerr constant polymer-stabilized blue phase liquid crystal" *Appl. Phys. Lett.* **98**, 081109 (2011).

[13] J. Yan, Y. Chen, S. T. Wu, S. H. Liu, K. L. Cheng, and J. W. Shiu, "Dynamic response of polymer-stabilized blue-phase liquid crystal," *J. Appl. Phys.* **111**, 063103 (2012).

[14] K. M. Chen, S. Gauza, H. Xianyu, and S. T. Wu, "Hysteresis effects in blue-phase liquid crystals," *J. Display Technol.* **6**, 318-322 (2010).

[15] L. Rao, J. Yan, S. T. Wu, Y. H. Chiu, H. Y. Chen, C. C. Liang, C. M. Wu, P. J. Hsieh, S. H. Liu, and K. L. Cheng, "Critical field for a hysteresis-free blue-phase liquid crystal device," *J. Display Technol.* **7**, 627-629 (2011).

[16] M. Jiao, J. Yan, and S. T. Wu, "Dispersion relation on the Kerr constant of a polymer-dispersed optically isotropic liquid crystal," *Phys. Rev. E* **83**, 041706 (2011).

[17] L. Rao, Z. Ge, S. T. Wu, and S. H. Lee, "Low voltage blue-phase liquid crystal displays," *Appl. Phys. Lett.* **95**, 231101 (2009).

[18] M. Kim, M. S. Kim, B. G. Kang, M. K. Kim, S. Yoon, S. H. Lee, Z. Ge, L. Rao, S. Gauza and S. T. Wu, "Wall-shaped electrodes for reducing the operation voltage of polymer-stabilized blue phase liquid crystal displays," *J. Phys. D: Appl. Phys.* **42**, 235502 (2009).

[19] S. Yoon, M. Kim, M. S. Kim, B. G. Kang, M. K. Kim, A. K. Srivastava, S. H. Lee, Z. Ge, L. Rao, S. Gauza, and S. T. Wu, "Optimization of electrode structure to improve the electro-optic characteristics of liquid crystal display based on Kerr effect," *Liq. Cryst.* **37**, 201-208 (2010).

[20] M. Jiao, Y. Li and S. T. Wu, "Low voltage and high transmittance blue-phase liquid crystal displays with corrugated electrodes," *Appl. Phys. Lett.* **96**, 011102 (2010).

[21] H. C. Cheng, J. Yan, T. Ishinabe, and S. T. Wu, "Vertical field switching for blue-phase liquid crystal devices," *Appl. Phys. Lett.* **98**, 261102 (2011).

[22] Y. H. Kim, S. T. Hur, C. S. Park, K. W. Park, S. W. Choi, S. W. Kang, and H. R. Kim, "A vertical-field-driven polymer-stabilized blue phase liquid crystal mode to obtain a higher transmittance and lower driving voltage," *Opt. Express* **29**, 17427-17438 (2011).

[23] H. C. Cheng, J. Yan, and S. T. Wu, "Wide-view vertical field switching blue phase liquid crystal displays," *J. Display Technol.* **8**, 627-633 (2012).

[24] Z. Ge, S. T. Wu, S. S. Kim, J. W. Park, and S. H. Lee, "Thin cell fringe field-switching liquid crystal display with a chiral dopant," *Appl. Phys. Lett.* **92**, 181109 (2008).

[25] K. M. Chen, J. Yan, S. T. Wu, Y. P. Chang, C. C. Tsai, and J. W. Shiu, "Electrode dimension effects on blue-phase liquid crystal displays," *J. Display Technol.*, **7**, 362-364 (2011).